Treatment Of Industrial Effluent By Synthesized Nano-Composite Zrcdpbo₄ Through Solar Energy

Saroj Lohar, Jeevan Kunwar Chouhan, Dushyant Kumar Prajapati,
Jinesh Menaria, Shipra Bhardwaj
Department of chemistry
Institution: government Meera Girls College, Mohan Lal Sukhadia University
Address: Udaipur, Rajasthan, India

Abstract: *Water is the most essential natural resource for living beings, animals and plants but unfortunately it is being polluted by various means. Coloured pollutants, mainly dyes contribute maximum to this. Thus an attempt is made to remove such pollutants in an eco-friendly manner. Novel nano sized composite material $ZrCdPbO_4$ is synthesized by coprecipitation method, characterized by UV-vis, IR, FESEM, XRD, XPS and EDX analysis methods and is used for removing such pollutants from water. The emphasis of the present work is to use the prepared material as photocatalyst for degradation of various pollutants. Experimental details of degradation of a common industrial effluent, Azure-A dye as role model are discussed. Number of factors are varied to obtain maximum degradation rate through pseudo first order kinetic study. Hydroxyl radicals are found to play important role in cleavage of various bonds of the pollutant and is endorsed by scavenger study. LCMS/MS analysis is carried to rule out the route of the degradation. Final products are ascertained by laboratory tests.*
Key Word: *degradation, hydroxyl radical, LCMS/MS analysis, photocatalyst, pseudo first order kinetics*

I. Introduction

Water is the essential natural resource for life on earth. Now a day, through release of different pollutants, the availability of potable water has decreased and if available, is adversely affecting the health of living beings. Some human activities like constructions, release of various industrial wastes like from yarn, paper, printing industries, agricultural and pharmaceutical waste, excavation, cutting of tree etc has harmed the nature and has disturbed the eco balance. One of such activities that had polluted water is synthesis of colours and dyes. These colour pollutants when excreted directly into water, without any treatment, cause harm to the resource ending into dangerous outcomes. Thus need of the hour is to treat such resources by any mean and remove these pollutants. Various treatment methods are available to treat pollutants in wastewater like foam separation, electrode materials, bio-adsorption technologies, Tailoring nanofiltration membranes, Fenton-flocculation process etc[1,2,3,4,5]. Beside these methods, photocatalysis has emerged as a modern technology for degradation of pollutants. Some pollutants like pharmaceuticals and diagnostic agents, different pesticides (alachlor, atrazine, chlorfenvinphos, diuron, isoproturon and pentachlorophenol), refractory organics, organic contaminants etc. are removed through such methods[6,7,8,9,10]. It was observed that photocatalytic degradation gives almost complete decolourization of dyes and removal of total organic carbon[11,12,13,14,15].

Various types of photocatalyst are synthesized and are found to have high degradation efficiency towards organic dyes. $Ca_4Fe_9O_{17}$, $CuInSe_2/TiO_2$ hybrid hetero-nanostructures, Fe_3O_4/ZnO nanoparticles, $CaMoO_4$/electroconductive geopolymer composite, $Fe_3O_4–TiO_2$, $CdBiYO_4$, tungsten containing nanoparticles etc are some examples of such photocatalysts [16,17,18,19,20,21,22]. Doping of photocatalysts was also found to enhance the rate of degradation like zinc sulfide doped with manganese, nickel and copper etc[23].

It is observed that hydroxyl radicals play a significant role in heterogeneous photocatalysis and in degradation of dyes[24,25]. Transition metal oxides like Al-based Fe_2O_3 nanostructures generate these radicals during photocatalysis[26]. The yield of hydroxyl radicals on photocatalyst surface was determined at the rate of 35.6 μM/hr, 0.28 μM/h and 0.88 μM/h for P25 (standard commercial catalysts), WO_3 and $Pt-C_3N_4$ photocatalysts respectively[27]. Photocatalytic system, $MoO_3/g-C_3N_4$ composite works in acidic medium which suggests the participation of superoxide radicals and holes instead of hydroxyl radicals[28]. Further pathways of degradation of dyes and intermediate molecules formed within the path were determined through study of peaks in LCMS/MS analysis[29,30,31,32,33]. Studies carried out with various types of doped transition metals were found to improve the photocatalytic activities especially in TiO_2[34,35]. The degradation study using $Li_2CuMo_2O_8$ as a photocatalyst was carried out[36].

Present investigations deal with synthesis, characterization and use of a novel nano composite material $ZrO_2.CdO.PbO$ as photocatalyst. Numerous beneficial properties of prepared photocatalyst makes it suitable for degradation of pollutants in water, especially dye molecules. Azure A dye was considered as a role model. Different factors like pH, dose of photocatalyst, concentration of dye, light intensity etc. were varied to extract the maximum degradation conditions. The reaction was observed to follow pseudo first order kinetics. Participation of hydroxyl free radical was ruled out by scavenger study. A tentative mechanism for degradation is proposed through LCMS/MS peak analysis and intermediates are also determined.

II. Material And Methods

Zirconyl nitrate, lead nitrate and cadmium nitrate were used as precursors (Merck) for synthesis of the photocatalyst, sodium hydroxide was used as precipitating agent (CDH) and Azure A (Otto) was used as the model pollutant. HCl (CDH) and NaOH (CDH) were used for adjusting the pH of the solutions and pH was recorded by pH meter (Hena imported pen type). Optical density of solutions at different time intervals was recorded by UV-Vis spectrophotometer (CHINO). A 200 Watt lamp (Philips) was used for irradiation and the intensity of light was measured by solarimeter (CEL-201). KI, EDTA and isopropyl alcohol (Merck) were used as scavenger to trap the active species. All chemicals were used in approximately 95-99% pure form and of LR grade. LCMS/MS technique on instrument XEVO-TQD#QCA1232 with ESI type, source temperature 144°C, mass range 125 to 1000, duration time 15 minutes and collision energy 3.0 was employed. The N2 adsorption isotherm, corresponding surface area and the pore parameter of the sample at liquid nitrogen temperature (77.35K) were recorded with B.E.T surface area analyzer (Model Nova 2200e, Quantachrome Instruments) by using multiple point BET method. TG-DTA-DTG analysis were performed in air, heating rate is 20°C/min on EXSTAR TG/DTA 6300 instrument in the temperature range of 0 to 800°C. Reference sample alumina powder was used for DTA analysis. LC/MS analysis for degradation of Azure A is carried out on instrument XEVO-TQD#QCA1232 with ESI type, source temperature 144°C, mass range 125 to 1000, duration time 15 minutes and collision energy 3.0.

Experimental

The photocatalyst $ZrCdPbO_4$ was synthesized by using precursors- zirconyl nitrate, lead nitrate and cadmium nitrate. Solid co-precipitation method was employed and sodium hydroxide was used as precipitating agent under controlled conditions. Solid off white coloured material was obtained after calcination with yield of 71.73 %. The material was then characterized by XRD to obtain crystal size of 21.59±6.15 nm, EDX analysis proved the presence of Zr, Cd, Pb and O elements in ratio 1:1:1:4, XPS analysis determined the oxidation states as +4 for Zirconium, +2 for cadmium, +2 for lead and -2 for oxygen. The molecular formula of the prepared photocatalyst was thus confirmed to be $ZrO2.CdO.PbO$. FE-SEM analysis showed homogeneous cluster form of the material and IR study showed bonding and vibrations (bending and stretching) correlated to CdO, PbO and ZrO_2 molecules. UV-Vis spectral study was used to determine the band gap and peak at 229 nm suggested it to be 5.0 eV. The results are reported earlier[37]. Larger band gap ensured higher photo-quantum efficiency of the prepared material because of greater life time of photo-generated electrons and holes, thus having enough time to degrade pollutants. Participation of OH free radical was ascertained by scavenger study. BET analysis and TG-DTA-DTG analysis were also carried out to determine the surface area and thermal stability of prepared material. The dye solution with pH 8.0, dose of photocatalyst 0.22 g, concentration of dye 0.2×10-4 M, was exposed to the light with intensity 74.0 mW/cm2 and 10 mL of the solution at different time intervals (7, 14 and 21 minutes) were quenched and separated from the reaction system. These samples were then subjected to LC-MS analysis.

III. Results and Discussion

Approximately 0.0416 g of powder sample was placed in a sample cell and allowed to degas at one of the degassing stations for three hours at 250°C in a vacuum degassing mode for BET analysis. The degassed sample was then subjected to analysis at one station and the data were recorded by admitting or removing a known quantity of adsorbing N_2 gas into and out of the sample cell containing the solid adsorbent maintained at constant temperature (77.35K). From the nitrogen adsorption isotherm the specific surface area was calculated using B.E.T equation (1)[38]. The pore parameter analysis was carried out with the help of DA (Dubinin-Astakhov), DR (Dubinin-Radushkevic) and BJH (Barrett- Joyner- Halenda) models.

$$\frac{1}{W[\left(\frac{P^0}{P}\right)-1]} = \frac{1}{W_m C} + \frac{C-1}{W_m C}\frac{P}{P^0} \quad \ldots\ldots\ldots (1)$$

With help of this equation total surface area of prepared material was calculated. A graph was plotted between $\frac{1}{W[\left(\frac{P^0}{P}\right)-1]}$ versus relative pressure P/P^0 as shown in figure 1. All observation data are summarized in table 1.
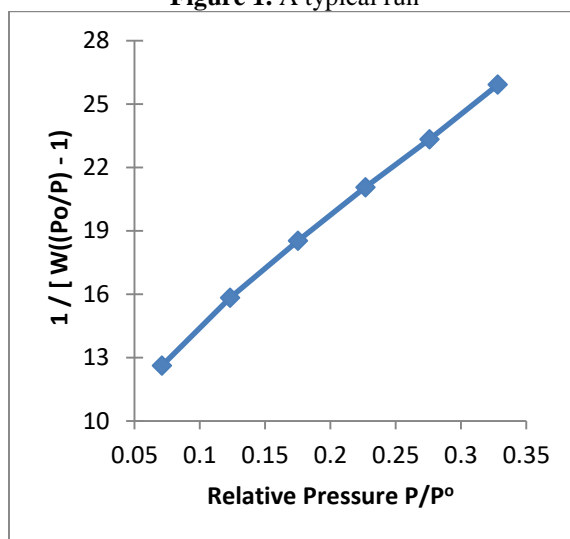
Figure 1. A typical run

Table 1 BET analysis data

BET constituents	Formula	Values
Slope	$S = \dfrac{C-1}{W_m C}$	51.008
Intercept	$I = \dfrac{1}{W_m C}$	9.348
Weight of the adsorbate	$W_m = \dfrac{1}{S+I}$	0.01656 g^{-1}
Total surface area	$S_t = \dfrac{W_m N A_{CS}}{M}$	57.70 m^{2}g^{-1}

Where N is Avogadro's number, A_{CS} is the cross sectional area, M is molecular weight of the adsorbate

An adsorption and desorption isotherm is shown in figure 2 which was plotted between volume and relative pressure. This isotherm corresponds to a type IV isotherm with H3 hysteresis loop[39]. Prepared material was found to have higher surface area of 57.00 m^{2}g^{-1} that is found beneficial for degrading organic pollutants with in lesser time span[40]. Further the analysis specified that the prepared material has mesoporous structure with pore diameter 3.396 nm[41].

Fig. 2 A adsorption and desorption isotherm
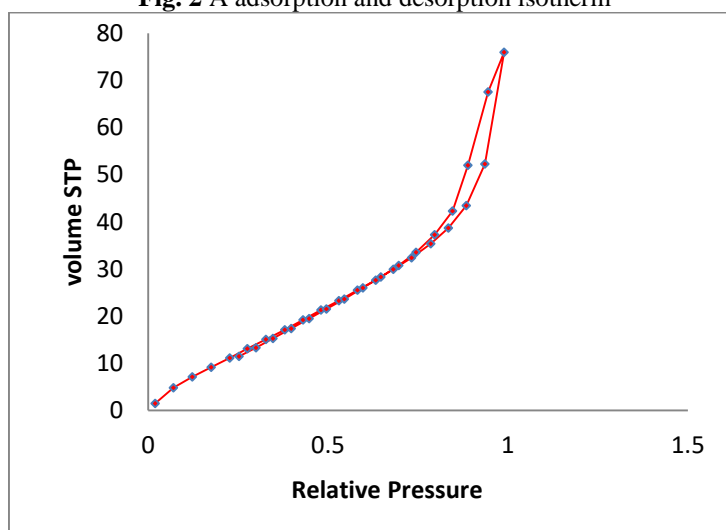
The Thermogram showed initial decomposition at 27°C and an endotherm peak at 97°C and DTG curve at 96°C. Total mass decay was 2.42 % at above temperature after complete exposure, 84.79% material was obtained suggesting high thermal stability of the photocatalyst. DTA peaks suggest endothermic reaction of the

decomposition. The prepared material has high thermally stable and it remains 84.79 % at 800 °C. Overall the decomposition was not observed for prepared material rather only impurities and gases were removed during the heat treatment through endothermic reactions. All observation data are summarized in table 2 and spectra in figure 3.
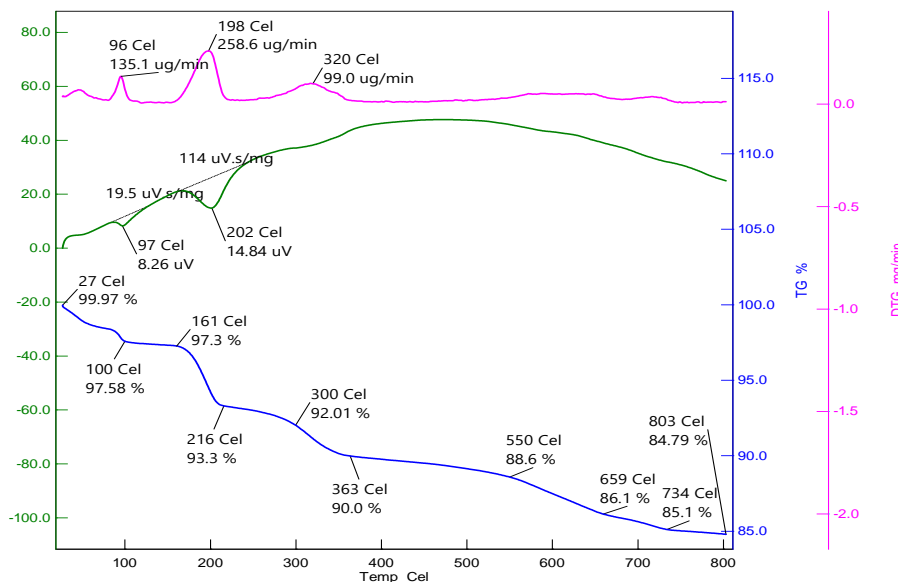
Figure 3. TG, DTG and DTA spectra

**Table 2.** TG, DTA and DTG peaks analysis data

Step	Temperature range (°C)	DTA (°C)	DTG (°C)	TG Residue (%)	Mass loss (%)
I	27-100	97 endothermic	96	97.58	2.42
II	161-216	202, endothermic	198	93.3	4.28
III	300-363	322, endothermic	320	90.0	3.3
IV	550-659	-	660	86.1	3.9
V	734-803	-	-	84.79	1.31

Further the photocatalyst was used for degradation of dye. Stock solution of the dye was prepared in doubly distilled water. Dye solution of concentration 0.2×10^{-4} M was taken, pH was adjusted to 8.0 and 0.22 g of $ZrCdPbO_4$ photocatalyst was added. The reaction mixture was then exposed to a tungsten lamp at the intensity of 74.0 mW/cm^2 and a water filter was used to cut off thermal side reactions. 2-3 mL of aliquot was drawn from the reaction mixture after particular time intervals during the progress of the reaction and optical density was recorded at λ_{max} 600 nm. It was observed that presence of light and the photocatalyst both were necessary to bring the degradation of dye, suggesting the reaction to be a photocatalytic one.

Typical Run

A typical run was plotted between 1+ log of optical density (O.D.) and time during the course of reaction. The observation data are graphically represented in figure 4. A straight line of the plot was observed. Kinetic models, pseudo-first-order and pseudo-second-order (Type-1, Type-2, Type-3, Type-4 and Type-5) were selected to explain the degradation data and it was found that pseudo-first-order kinetic model prevailed in degradation process[42]. Maximum degradation of the dye Azure A was attained at pH 8.0, dose of photocatalyst 0.22 g, concentration of Azure A 0.2×10^{-4} M and light intensity 74.0 mW/cm^2.

Figure 4. A typical run
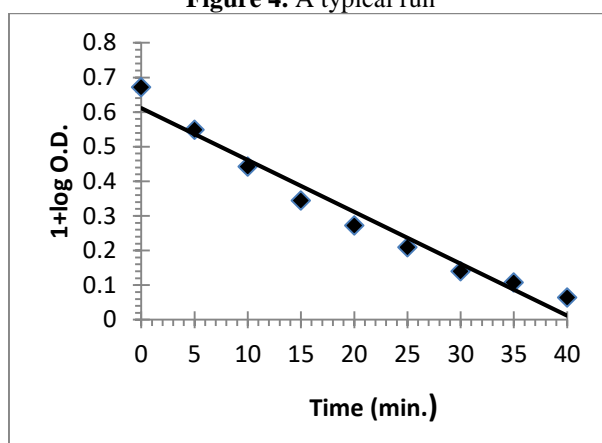
Nearly 75.31% dye concentration was degraded within 40 minutes of the exposure to light.

Degradation Efficiency (DE) (%) $= \frac{A_0 - A_t}{A_0} \times 100 = 75.31\%$

Degradation is found to be k= 7.67×10^{-4} (sec^{-1}). Reaction conditions were varied to obtain maximum degradation as follows:-

pH variation

One of the major factors affecting the rate of degradation of the dye is pH of the solution as dyes are sensitive towards change in pH. Some dyes even change their colour on change in pH. Thus it was varied and all other factors were kept constant. It was observed that with change in pH, the initial optical density of the solution changes, which can also be observed in multiline graphs. The effect of pH was studied in range 5.0 to 10.0 with difference of 0.5 and results are reported in figure 5.

Figure 5. Effect of variation of pH
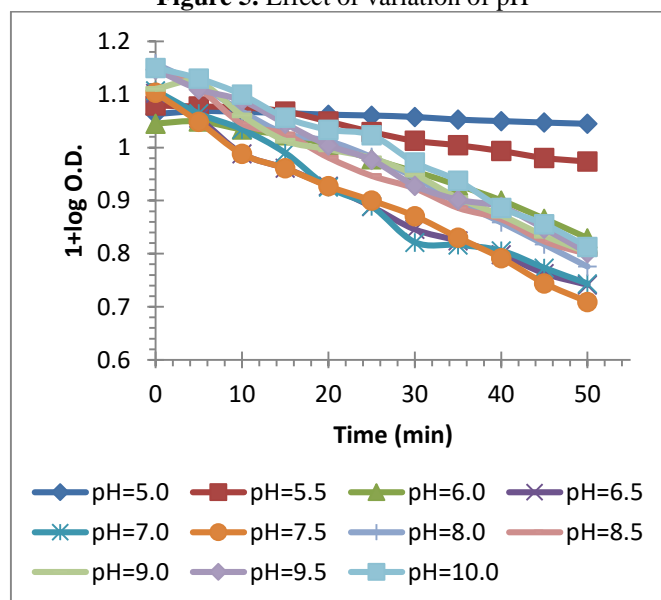
It was observed that rate of photocatalytic degradation increased with increase in pH up to 8.0 and then gradually decreased. The reason behind is generation of more electron hole pairs at photocatalyst surface by absorption of photons

$ZrCdPbO_4 + h\nu \rightarrow [e^-_{(CB)} + h^+_{(VB)}]$

(Electron-hole pair formation)   (2)

The increase in rate of degradation upto pH 8.0, is attributed to the availability of more concentration of OH$^-$ ions in the solution which loose their electrons to holes, generating hydroxyl free radicals and which are the responsible species causing degradation.

$h^+_{(VB)} + OH^- \rightarrow {}^\bullet OH$

(Radical formation)   (3)

After pH 8.0, decrease in reaction rate is observed due to repulsion amongst OH^- ions and electrons on photocatalyst surface causing the recombination of electrons and holes, besides abstracting electrons from OH^- species. Thus a decrease in the rate of degradation is observed.

Scavenger study is carried out to find out the role of active species that caused the degradation of dye molecules. Various scavengers benzoquinone, EDTA, KI and isopropyl alcohol were used and are graphically reported in figure 6. It is evident from the data that addition of isopropyl alcohol (hydroxyl radical scavenger) ceases the reaction and significant reduces the rate of degradation (up to 82%) thus proving the participation of ˙OH free radicals as active species in degradation of the dye molecules.

Figure 6. Scavenger study
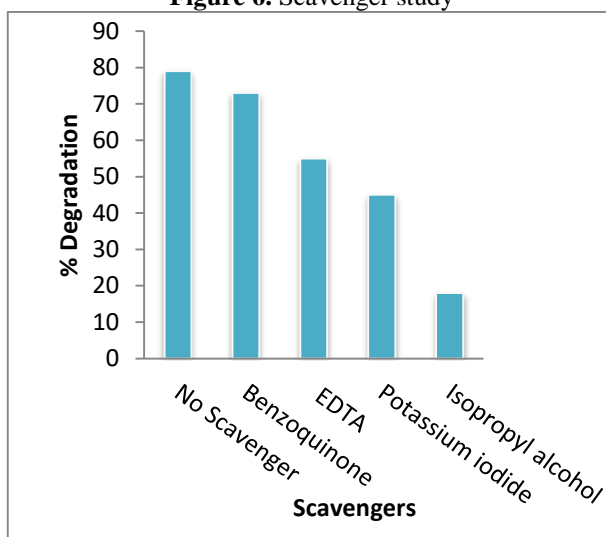
Dose of Photocatalyst Variation

The effect of dose of photocatalyst was studied by varying its weight and with keeping all other factors constant. Figure 7 represents the effect graphically.

Maximum rate of degradation was observed at 0.22 g of photocatalyst. Further increase in dose of photocatalyst, reduced the rate of reaction. It is explained on the basis that with increase in dose of photocatalyst surface area of particles exposed to light increases and thus formation of number of electron-hole pairs increases. Electrons from this pair cause reduction whereas holes are responsible for causing oxidation as these abstract electrons from the OH^- ions producing ˙OH free radicals and from the dye molecules causing degradation. Scavenger study suggests the participation of ˙OH free radicals as the species responsible for degradation of dye molecules. Thus increase in rate is observed. After attaining maximum value (at 0.22g), rate of reaction decreases due to formation of multilayer of photocatalyst that forces the recombination of generated electrons and holes lowering rate of reaction.

Figure 7. Effect of variation of dose of photocatalyst
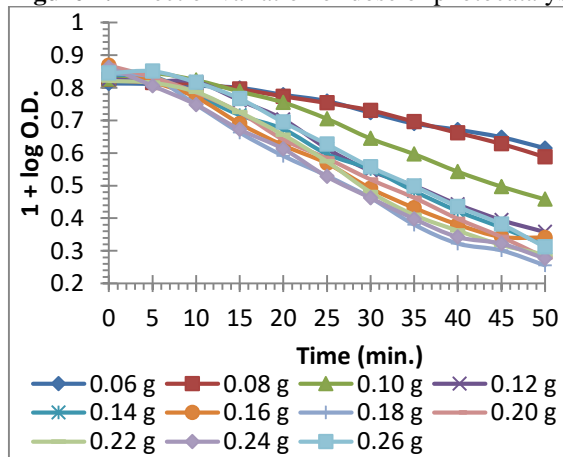
Dye Concentration variation

The effect of concentration of dye on degradation was studied and the resulting data are shown graphically in figure 8. All other factors were kept constant. Dye molecules absorb the light radiations and get excited to singlet state during the reaction which converts to triplet state by inter system crossing.

Dye + hv (Photons) → Dye^1

(Singlet excited state) (4)

Dye^1 → Dye^3

(Triplet excited state) (5)
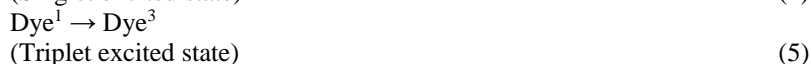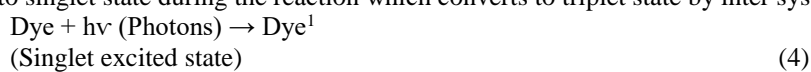
Those dye molecules are then attacked by OH free radicals at weaker bond site and breakdown of the molecules is observed.

$^{\bullet}$OH + Dye^3 → Leuco Dye → Degraded Products (6)

The study reveals that rate of reaction increases with increase in concentration of dye. The reason is with increase in concentration, more dye molecules are available to absorb photons from light and get excited. Thus rate of degradation increases. After attaining maximum value (at 0.2×10^{-4} M), increase in concentration of the dye decreases the rate of degradation as beyond the concentration, addition of dye solution imparts darker colour to the reaction mixture and starts acting as filter to the incident light. Thus the desired amount of incident light does not reach the photocatalyst surface and as a result the rate of reaction decreases.

**Figure 8.** Effect of variation of dye concentration (Moles/Litre)
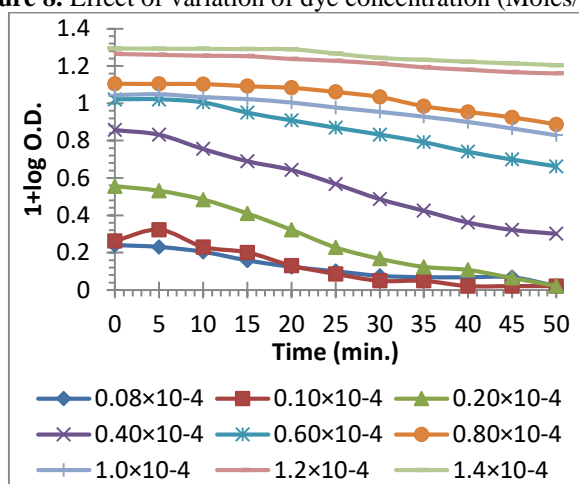
Exposure to Light

Light intensity was varied out in the range 7.0 to 74.0 mW/cm^2 data of which are graphically represented in figure 9. All other factors were kept constant.

It was observed that the rate of photocatalytic degradation increased with the intensity of light. This is explained by the fact that with increase in light intensity, number of photons striking per unit area per unit time increases. This increases the number of excited dye molecules and electron hole pair at the surface of photocatalyst. The rate of degradation is found maximum at light intensity 74.0 mW/cm^2. Further increase in intensity of light causes heating of the solution and thus is avoided.

Figure 9. Effect of variation of light intensity (mW/cm^2)
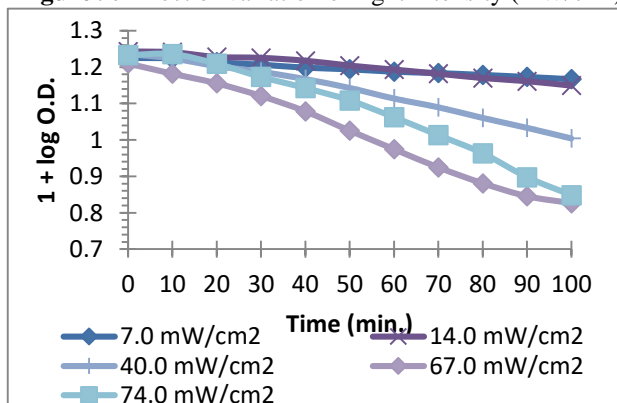
LCMS/MS Analysis for Determination of Degradation Pathway

Liquid Chromatography-Tandem Mass Spectrometry (LC-MS/MS) is an analytical method in which fragmentation of any molecule is analyzed by trapping separated ions[43]. The mechanistic path in degradation of dyes like Methylene Blue, Orange G etc was studied using LCMS technique [44,45,46,47,48].

LC-MS analysis of the sample drawn after different time intervals was carried out. The data are given in table 3 and peaks are observed in figure 10. The values of m/z were calculated to obtain possible degradation pathway and tentative fragmentation of dye molecule which are observed in scheme 1. Further formation of smaller gaseous fragments were ascertained through laboratory experiments.

Table 3. Mass to charge ratio in LC-MS/MS spectra during cleavage of Azure A

Structure no.	Chemical Formula	Exact Mass	MS/MS Fragments	% Mass Error
1	$C_{14}H_{14}ClN_3S$	291.06	289.3	0.99
2	$C_{14}H_{14}N_3S^+$	256.09	257.3	1.00
3	$C_{12}H_{10}N_3S^+$	228.07	229.2	1.00
4	$C_{12}H_{13}N_3O_5S$	311.06	311.1	1.00
5	$C_6H_9NO_5S$	207.02	203.2	0.98
5'	$C_6H_8N_2O_5S$	220.02	221.2	1.00
5''	$C_6H_{15}NO_5$	181.09	185.3	1.02
6	$C_6H_8N_2O_3$	156.05	159.1	1.01
6'	$C_6H_7NO_2$	125.05	130.3	1.04
7	$C_6H_6N_2O_2$	154.03	159.1	1.03
7'	$C_6H_9NO_4S$	191.03	195.2	1.02
8	$C_6H_{10}N_2O_3$	158.06	164.1	0.96
8'	$C_6H_{11}NO_5S$	209.03	210.1	1.00

LC/MS peak analysis suggested that during degradation process, the dye molecules are attacked by ˙OH free radicals several times, at the weaker bond site and a breakdown of ring as well as of conjugation is observed resulting in formation of smaller fragments.

Initially the removal of halogen molecule and demethylation process occurs and then formation of thionine molecule which is attacked by hydroxyl free radicals and generates molecule 4 (m/z 311.05 via 2 and 3 of m/z 257 and 229 respectively, figure 10b). Further attack results in breakdown of the central ring into two fragments 5 and 6 (m/z 203.2 and 159.1 respectively, figure 10a, 10c). Molecule 5 is further attacked by hydroxyl free radicals converting into 5'' (m/z 185.3, figure 10c) and total double bond break down (TDBB) is observed to form smaller molecules. Molecule 5 also gets converted to molecule 6 and further attack of ˙OH free radicals causes removal of H_2O from the unstable fragment producing molecule 7 (m/z 159.1) followed by break down of ringed species to form molecule 8 (m/z 160, figure 10c) and into smaller fragments like CO_2, NH_3, H_2O etc is observed.

Simultaneously, following other path, molecule 4 breaks into two fragments that are molecule 5' (m/z 221.2) and molecule 6' (m/z 130.3, figure 10a, 10c). Molecule 5' then gets converted to molecule 7' (m/z 195.2) via molecule 6', by removal of unstable fragment (figure 10b). Further attack of free radical breaks the ring to form molecule 8' (m/z 210.1). Elemental test in the residual solution proved that no element is left behind, suggesting complete breakdown of the dye molecules in smaller fragments like CO_2, SO_2, NO_2, NH_3, H_2O etc.

**Scheme 1.** Mechanistic pathway proposed for degradation of Azure A
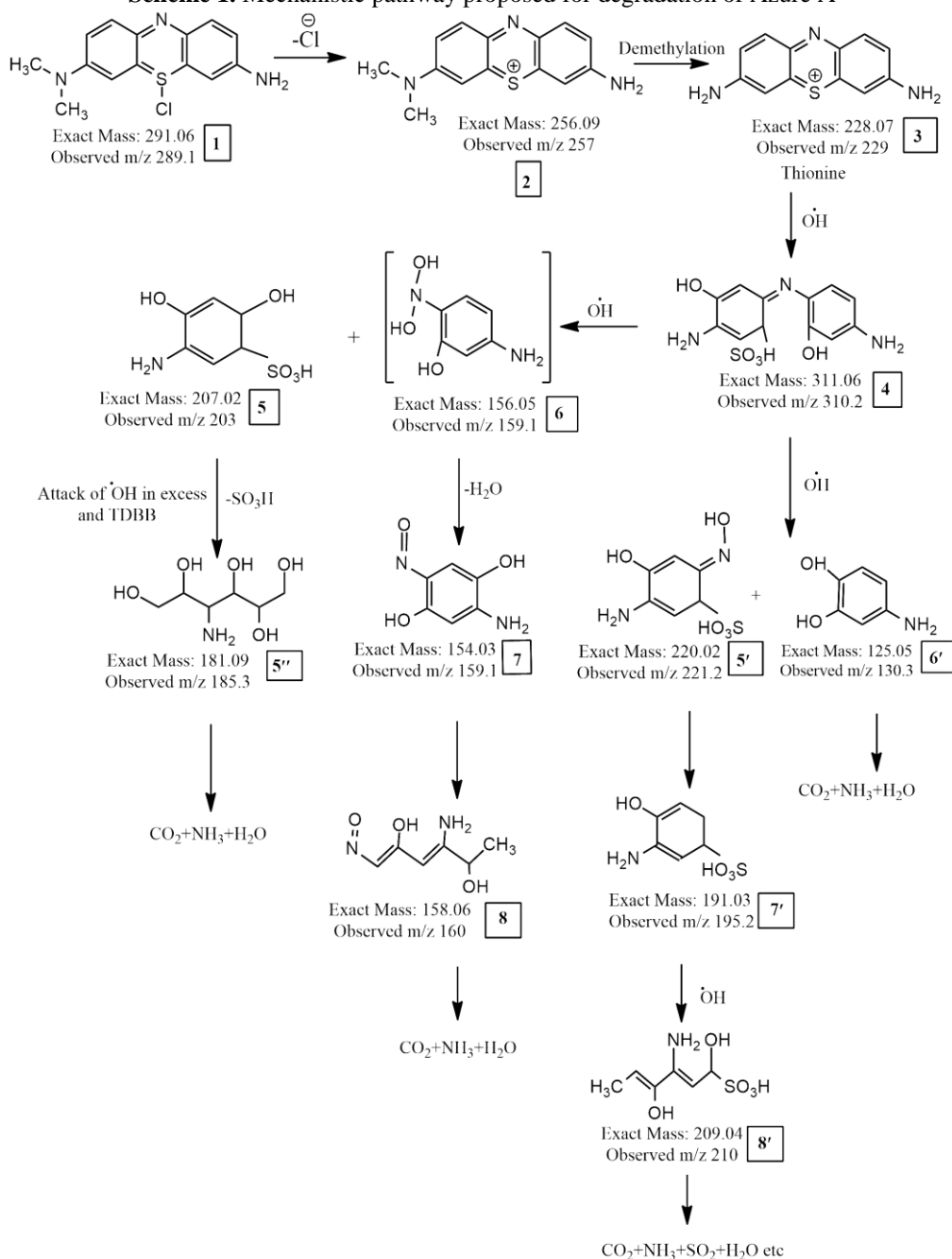
Numbers of peak are observed at higher m/z values suggesting the formation of unstable polymeric molecules by recombination of fragments which readily break down into smaller ones. A tentative route is drawn for the same (scheme 2). Some molecules with higher mass values 349, 456,762, 963 etc are constructed through azo linkage, ether linkage and through release of small fragments like H_2O, CO_2, H_2 etc. Lower intensity of these peaks suggested their lower stability (figure 11) and their instantaneous breakdown into other fragments.

Figure11. LCMS spectra of Azure A cleavage and peaks at higher m/z
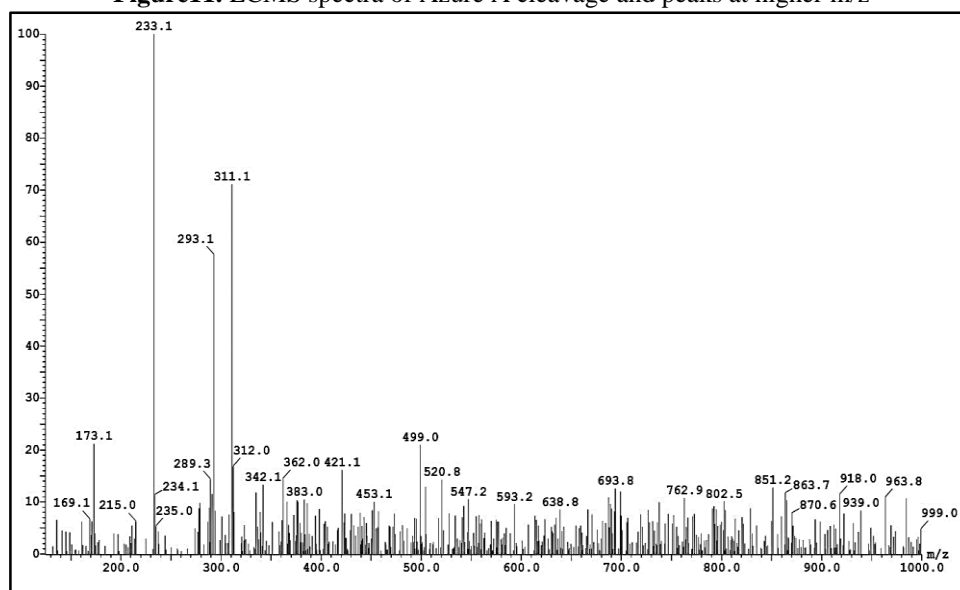
Scheme 2. Mechanistic pathway of intermediates with high molecular mass fragments
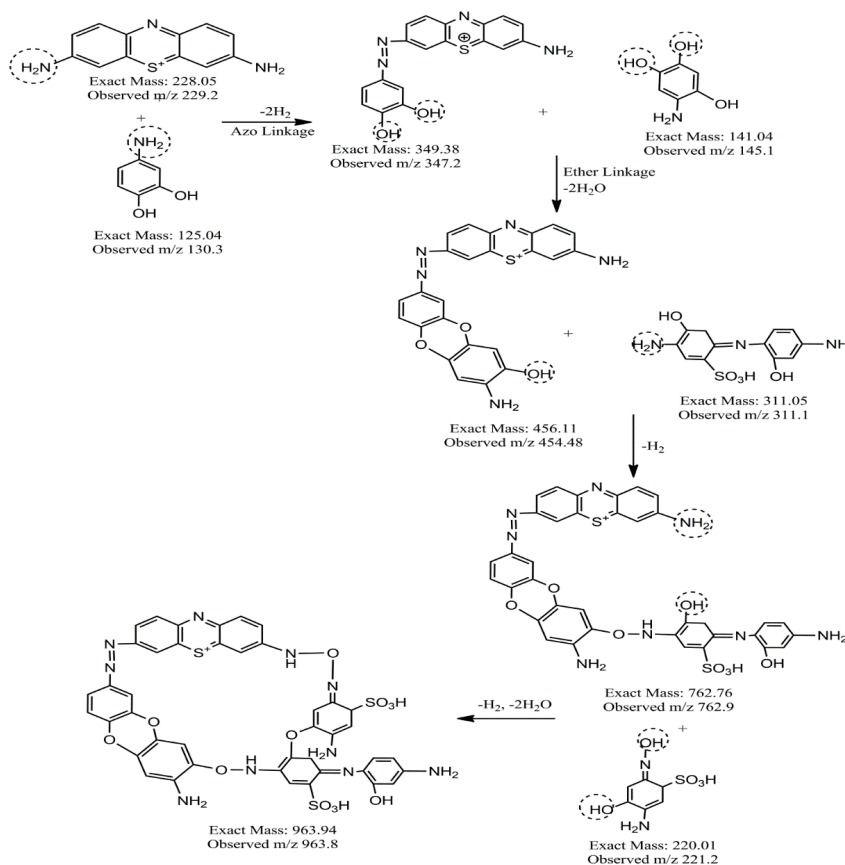
IV. Conclusion

It is concluded here by that a novel nanosized quaternary photocatalyst is synthesized and is characterized. Band gap energy of the photocatalyst comes out to be 5 eV, which makes the material suitable for photocatalytic activities as recombination of electrons and holes is reduced. The photocatalyst is further used for removal of dye Azure A from water. A mechanistic pathway is proposed where degraded fragments are identified by considering m/z peaks through LC-MS spectra. Complete degradation of the dye molecules into smaller harmless fragments is observed. The process is found beneficial for the society in numerous ways. Use of solar radiations, simple process of regeneration and reusability of photocatalyst, treatment of polluted water to make it

useful, less time and energy consuming process etc. makes the process economic one. The process does not add any other material to the resource or environment and so is an eco-friendly process. Thus the process can be used at larger scale for purification of water.

Acknowledgements

<div align="center">References</div>

[1]. X. Fei, W. Li, S. Zhu, L. Liu, Y. Yang. Simultaneous Treatment Of Dye Wastewater And Surfactant Wastewater By Foam Separation: Experimental And Mesoscopic Simulation Study. Sep. Sci. Technol., 53, 2018, 1604-1610. Doi: 10.1080/01496395.2017.1406951

[2]. J. Yang, Y. Yang, A. Li, Z. Wang, H. Wang, D. Yu, P. Hu, M. Qian, J. Lin, L. Guo. Sustainable Treatment Of Dye Wastewater For High-Performance Rechargeable Battery Cathodes. Energy Storage Mater., 17, 2019, 334-340.

[3]. W. Li, B. Mu, Y. Yang. Feasibility Of Industrial-Scale Treatment Of Dye Wastewater Via Bio-Adsorption Technology. Bioresource Technol., 277, 2019, 157-170.

[4]. X. Cao, Y. Yan, F. Zhou, S. Sun. Tailoring Nanofiltration Membranes For Effective Removing Dye Intermediates In Complex Dye-Wastewater. J. Membrane Sci., 595, 2020, 117476.

[5]. X. Xiao, Y. Sun, W. Sun, H. Shen, H. Zheng, Y. Xu, J. Zhao, H. Wu, C. Liu. Advanced Treatment Of Actual Textile Dye Wastewater By Fenton-Flocculation Process. Can. J. Chem. Eng., 95, 2017, 1245-1252. Https://Doi.Org/10.1002/Cjce.22752

[6]. T.E. Doll, F.H. Frimmel. Removal Of Selected Persistent Organic Pollutants By Heterogeneous Photocatalysis In Water. Catal. Today, 101, 2005, 195-202.

[7]. M. Hincapie, M.I. Maldonado, I. Oller, W. Gernjak, J.A. Sanchez-Perez, M.M. Ballesteros, S. Malato,.Solar Photocatalytic Degradation And Detoxification Of Eu Priority Substances. Catal. Today, 101, 2005, 203-210.

[8]. J. Xiao, Y. Xie, H. Cao. Organic Pollutants Removal In Wastewater By Heterogeneous Photocatalytic Ozonation. Chemosphere, 121, 2015, 1-17.

[9]. E. Pelizzetti, C. Minero. Mechanism Of The Photo-Oxidative Degradation Of Organic Pollutants Over TiO_2 Particles. Electrochimica Acta, 38, 2015, 47-55.

[10]. V. Goetz, J.P. Cambon, D. Sacco, G. Plantard. Modeling Aqueous Heterogeneous Photocatalytic Degradation Of Organic Pollutants With Immobilized TiO_2. Chem. Eng. Process: Process Intensification, 48, 2009, 532-537.

[11]. C. Gouvêa, F. Wypych, S.G. Moraes, N. Durán, N. Nagata, P. Peralta-Zamora. Semiconductor-Assisted Photocatalytic Degradation Of Reactive Dyes In Aqueous Solution. Chemosphere, 40, 2000, 433-440.

[12]. C. Kuo. Prevenient Dye-Degradation Mechanisms Using Uv/TiO_2/Carbon Nanotubes Process. J. Hazard. Mater., 163, 2009, 239-244.

[13]. E. Bizani, K. Fytianos, I. Poulios, V. Tsiridis. Photocatalytic Decolorization And Degradation Of Dye Solutions And Wastewaters In The Presence Of Titanium Dioxide. J. Hazard. Mater., 136, 2006, 85-94.

[14]. C. Andriantsiferana, E.F. Mohamed, H. Delmas. Photocatalytic Degradation Of An Azo-Dye On TiO_2/Activated Carbon Composite Material. Environ. Technol., 35, 2014, 355-363. Doi: 10.1080/09593330.2013.828094

[15]. O. Sacco, M. Stoller, V. Vaiano, P. Ciambelli, A. Chianese, D. Sannino. Photocatalytic Degradation Of Organic Dyes Under Visible Light On N-Doped TiO_2 Photocatalysts. Inter. J. Photoenergy Article Id 626759, 2012, 8 Pages Doi:10.1155/2012/626759

[16]. P. Chatterjee, A.K. Chakraborty. Metal Organic Framework Derived $Ca_4fe_9O_{17}$ As Photocatalyst For Degradation Of Organic Dyes. Mater. Letters, 284, 2021, 129034.

[17]. A.S. Kshirsagar, A. Gautam, P.K. Khanna. Efficient Photo-Catalytic Oxidative Degradation Of Organic Dyes Using $Cuinse_2/TiO_2$ Hybrid Hetero-Nanostructures. J. Photochem. Photobiol. A: Chem., 349, 2017, 73-90.

[18]. O. Długosz, K. Szostak, M. Krupiński, M. Banach. Synthesis Of Fe_3O_4/Zno Nanoparticles And Their Application For The Photodegradation Of Anionic And Cationic Dyes. Int. J. Environ. Sci. Technol., 18, 2021, 561–574.

[19]. P.Y. He, Y.J. Zhang, H. Chen, L.C. Liu. Development Of An Eco-Efficient $Camoo_4$/Electroconductive Geopolymer Composite For Recycling Silicomanganese Slag And Degradation Of Dye Wastewater. J. Cleaner Production, 208, 2019, 1476-1487.

[20]. M.A. Zazouli, F. Ghanbari, M. Yousefi, S. Madihi-Bidgoli. Photocatalytic Degradation Of Food Dye By $Fe_3O_4–TiO_2$ Nanoparticles In Presence Of Peroxymonosulfate: The Effect Of Uv Sources. J. Environ. Chem. Eng., 5, 2017, 2459-2468.

[21]. H. Du, J. Luan. Synthesis, Characterization And Photocatalytic Activity Of New Photocatalyst $Cdbiyo_4$. Solid State Sci., 14, 2012, 1295-1305.

[22]. Vijay, S. Bhardwaj. A Comparative Study Of Photocatalytic Degradation Of Azure-B By Tungsten Containing Nanoparticles: Sunlight Used As Energy Source. J. App. Chem., 8, 2015, 66-72.

[23]. H.R. Poureredal, A. Norozi, M.H. Keshavarz, A. Semnani. Nanoparticles Of Zinc Sulfide Doped With Manganese, Nickel And Copper As Nanophotocatalyst In The Degradation Of Organic Dyes. J. Hazard. Mater., 162, 2009, 674-681.

[24]. N. Daneshvar, D. Salari, A.R. Khataee. Photocatalytic Degradation Of Azo Dye Acid Red 14 In Water On Zno As An Alternative Catalyst To TiO_2. J. Photochem. Photobiol. A: Chem., 162, 2004, 317-322.

[25]. P. Raizada, P. Singh, A. Kumar, G. Sharma, B. Pare, S.B. Jonnalagadda, P. Thakur. Solar Photocatalytic Activity Of Nano-Zno Supported On Activated Carbon Or Brick Grain Particles: Role Of Adsorption In Dye Degradation. Appl. Catal. A: General, 486, 2014,159-169.

[26]. S.S. Shinde, C.H. Bhosale, K.Y. Rajpure. Kinetic Analysis Of Heterogeneous Pohotocatalysis: Role Of Hydroxyl Radicals. Catal. Rev., 55, 2013, 79-133. Doi: 10.1080/01614940.2012.734202

[27]. S. Nagarajan, N.C. Skillen, F. Fina, G. Zhang, C. Randorn, L.A. Lawton, J. Irvine, P. Robertson. Comparative Assessment Of Visible Light And Uv Active Photocatalysts By Hydroxyl Radical Quantification. J. Photochem. Photobiol. A: Chem., 334, 2017, 13-19.

[28]. S. Xue, S. Wu, S. Pu, Y. Hou, T. Tong, G. Yang, Z. Qin, Z. Wang, J. Bao. Direct Z-Scheme Charge Transfer In Heterostructured $Moo_3/G-C_3n_4$ Photocatalysts And The Generation Of Active Radicals In Photocatalytic Dye Degradations. Environ. Pollution, 250, 2019, 338-345.

[29]. J. Shen, Z. Jiang, D. Liao, J. Horng. Enhanced Synergistic Photocatalytic Activity Of TiO_2/Oxidant For Azo Dye Degradation Under Simulated Solar Irradiation: A Determination Of Product Formation Regularity By Quantifying Hydroxyl Radical-Reacted Efficiency. J. Water Process. Eng., 40, 2021, 101893.

[30]. H.E. Zhong, Y. Shaogui, J.U. Yongming, S. Cheng. Microwave Photocatalytic Degradation Of Rhodamine B Using TiO_2 Supported On Activated Carbon: Mechanism Implication. J. Environ. Sci., 21, 2009, 268-272.

[31].   H. Mittal, M. Khanuja. Optimization Of Mose$_2$ Nanostructure By Surface Modification Using Conducting Polymer For Degradation Of Cationic And Anionic Dye: Photocatalysis Mechanism, Reaction Kinetics And Intermediate Product Study. Dyes Pig., 175, 2020, 108109.

[32].   Z. Chen, D. Li, W. Zhang, Y. Shao, T. Chen, M. Sun, X. Fu. Photocatalytic Degradation Of Dyes By Znin$_2$s$_4$ Microspheres Under Visible Light Irradiation. J. Phys. Chem. C, 113, 2009, 4433-4440. Doi: 10.1021/Jp8092513

[33].   W.K. Jo, T. Adinaveen, J.J. Vijaya, N. Selvam. Synthesis Of Mos$_2$ Nanosheet Supported Z-Scheme Tio$_2$/G-C$_3$n$_4$ Photocatalysts For The Enhanced Photocatalytic Degradation Of Organic Water Pollutants. Rsc Adv., 6, 2016, 10487-10497.

[34].   E.B. Gracien, J. Shen, X. Sun, D. Liu, M. Li, S. Yao, J. Sun. Photocatalytic Activity Of Manganese, Chromium And Cobalt-Doped Anatase Titanium Dioxide Nanoporous Electrodes Produced By Re-Anodization Method. Thin Solid Films, 515, 2007, 5287–5297.

[35].   R. Wong, J. Feng, X. Hu, P.L. Yue. Discoloration And Mineralization Of Non-Biodegradable Azo Dye Orange Ii By Copper-Doped Tio$_2$ Nanocatalysts. J. Environ. Sci. Health Part A: Toxic/Hazard. Subst. Environ. Eng., 39, 2005, 2583–2595.

[36].   M. Joshi, P. Kumawat, R. Ameta, S.C. Ameta. Photocatalytic Mineralization Of Azure A Using Li$_2$cumo$_2$o$_8$ Nanoparticles. Inter. J. Res. Chem. Environ., 5, 2015, 103-109.

[37].   S. Lohar, A. Vijay, S. Bhardwaj. Removal Of Organic Pollutants By Zirconium Containing Nanoparticles: A Comparative Photocatalytic Degradation Study. J. Mater. Sci.: Mater. Electron., 32, 2021, 12424–12438. Https://Doi.Org/10.1007/S10854-021-05874-X

[38].   I.A. Wani, S. Khatoon, A. Ganguly, J. Ahmed, A.K. Ganguli, T. Ahmad. Silver Nanoparticles: Large Scale Solvothermal Synthesis And Optical Properties, Mater. Res. Bulletin, 45, 2008, 1033-1038. Doi:10.1016/J.Materresbull.2010.03.028.

[39].   S. Adhikari, D. Sarkar, G. Madras. Hierarchical Design Of Cus Architectures For Visible Light Photocatalysis Of 4-Chlorophenol. Acs Omega, 2, 2017, 4009−4021.

[40].   Kumar, A. Rana, C. Guo, G. Sharma, K.M. Katubi, F.M. Alzahrani, M. Naushad, M. Sillanpää, P. Dhiman, F.J. Stadler . Acceleration Of Photo-Reduction And Oxidation Capabilities Of Bi$_4$o$_5$i$_2$/Spion@Calcium Alginate By Metallic Ag: Wide Spectral Removal Of Nitrate And Azithromycin. Chem. Eng. J., 423, 2021, 130173.

[41].   J. Rouquerol, D. Avnir, C.W. Fairbridge, D.H. Everett, J.M. Haynes, N. Pernicone, J.D. Ramsay, K.S. Sing, K.K. Unger . Recommendations For The Characterization Of Porous Solids (Technical Report). Pure Appl. Chem., 66, 1994, 1739-1758. Https://Doi.Org/10.1351/Pac199466081739

[42].   M. Zulfiqar, S. Sufian, N. Mansor, N.E. Rabat. Synthesis And Characterization Of Tio$_2$-Based Nanostructures Via Fluorine-Free Solvothermal Method For Enhancing Visible Light Photocatalytic Activity: Experimental And Theoretical Approach. J. Photochem. Photobiol. A: Chem., 404, 2021, 112834. Https://Doi.Org/10.1016/J.Jphotochem.2020.112834

[43].   T. Chen, Y. Zheng, J.M. Lin, G. Chen. Study On The Photocatalytic Degradation Of Methyl Orange In Water Using Ag/Zno As Catalyst By Liquid Chromatography Electrospray Ionization Ion-Trap Mass Spectrometry. J. Am. Soc. Mass Spectrom., 19, 2008, 997–1003.

[44].   M.A. Rauf, M.A. Meetani, A. Khaleel, A. Ahmed. Photocatalytic Degradation Of Methylene Blue Using A Mixed Catalyst And Product Analysis By Lc/Ms. Chem., Eng. J., 157, 2010, 373–378.

[45].   M.A. Meetani, M.A. Rauf, S. Hisaindee, A. Khaleel, A. Alzamly, A. Ahmad. Mechanistic Studies Of Photoinduced Degradation Of Orange G Using Lc/Ms. Rsc Adv., 1, 2011, 490–497.

[46].   S. Hisaindee, M.A. Meetani, M.A. Rauf. Application Of Lc-Ms To The Analysis Of Advanced Oxidation Process (Aop) Degradation Of Dye Products And Reaction Mechanisms. Trends Anal. Chem., 49, 2013, 31–44.

[47].   R. Kushwaha, S. Garg, S. Bajpai, A.S. Giri. Degradation Of Nile Blue Sulphate Dye Onto Iron Oxide Nanoparticles: Kinetic Study, Identification Of Reaction Intermediates, And Proposed Mechanistic Pathways. Asia-Pac. J. Chem. Eng., 2018, 2200. Https://Doi.Org/10.1002/Apj.2200

[48].   T. Sinha, M. Ahmaruzzaman. Green Synthesis Of Copper Nanoparticles For The Efficient Removal (Degradation) Of Dye From Aqueous Phase. Environ. Sci. Pollut. Res., 22, 2015, 20092-20100. Doi 10.1007/S11356-015-5223-Y.